Research Square

Preprints are preliminary reports that have not undergone peer review.
They should not be considered conclusive, used to inform clinical practice,
or referenced by the media as validated information.

Collapse misclassification dominates the uncertainty in city-scale earthquake fatality estimates: a validated probabilistic seismic risk model for the residential building stock of Peshawar, Pakistan

Wasim Khan
University of Engineering and Technology Peshawar
Shahid Ullah
shahid.ullah@uetpeshawar.edu.pk
University of Engineering and Technology Peshawar
Huma Aman
University of Engineering and Technology Peshawar

Research Article

Keywords: Probabilistic seismic risk, Epistemic uncertainty, Earthquake casualties, Unreinforced masonry, OpenQuake, Pakistan

Posted Date: November 16th, 2026

DOI: https://doi.org/10.21203/rs.3.rs-11492895/v1

License: This work is licensed under a Creative Commons Attribution 4.0 International License.
Read Full License

Additional Declarations: No competing interests reported.

Collapse misclassification dominates the uncertainty in city-scale earthquake fatality estimates: a validated probabilistic seismic risk model for the residential building stock of Peshawar, Pakistan

Wasim Khan[1] , Shahid Ullah[1*] , Huma Aman[1]

[1] Earthquake Engineering Center, Department of Civil Engineering, University of Engineering and Technology Peshawar, Peshawar 25120, Khyber Pakhtunkhwa, Pakistan

Corresponding author: Shahid Ullah, shahid.ullah@uetpeshawar.edu.pk

Abstract

Probabilistic seismic risk estimates for rapidly growing cities in data-scarce regions are increasingly used to set mitigation priorities, yet the fatality component of these estimates is rarely tested. This study develops an updated event-based seismic risk model for the residential building stock of District Peshawar, Pakistan (361,357 buildings; 4.31 million people; USD 7.83 billion replacement value), using the seismic source model of the 2021 Building Code of Pakistan, a census-based exposure model mapped to seven Global Earthquake Model (GEM) building classes, and GEM analytical fragility functions. A hazard-consistent closed-form model is then derived by inverting the event-based aggregate loss curve into an equivalent spectral-acceleration hazard curve. The closed-form model reproduces the event-based average annual loss (AAL), and its 475- and 2,475-year intensities agree with the building-code hazard and 13 published hazard studies. The baseline AAL is USD 20.2 to 22.8 million (0.26 to 0.29% of replacement value), and unreinforced brick and adobe masonry account for 97% of it. Fatality estimates, however, depend critically on how the complete-damage state is translated into casualties. Treating every completely damaged building as collapsed, as is common in practice, yields 412 to 881 deaths per year, which, in a back-analysis of the 2015 Mw 7.5 Hindu Kush earthquake, can exceed the death toll of the entire province. Applying HAZUS collapse fractions, or GEM fatality vulnerability functions, reduces the estimate to 51 to 77 deaths per year (1.2 to 1.8 per 100,000) and reconciles the model with the 2015 observations. A nine-factor sensitivity analysis and a 1,500-run Monte Carlo propagation show that the casualty model, the hazard level and the collapse lethality dominate the uncertainty in fatalities (5 to 95% range 18 to 259 per year), whereas the choice of vulnerability model dominates AAL. Retrofitting single-storey adobe houses is five to six times more cost-effective per life saved than retrofitting brick masonry, although no strategy is economically justified on direct losses alone.

Keywords Probabilistic seismic risk · Epistemic uncertainty · Earthquake casualties · Unreinforced masonry · OpenQuake · Pakistan

1 Introduction

Pakistan lies at the junction of the Indian, Eurasian and Arabian plates, and damaging earthquakes of magnitude 7 or greater have historically affected the country roughly once per decade (Bilham 2009; Ahmad et al. 2014). The devastating 2005 Kashmir earthquake triggered a national shift from post-disaster response towards risk-informed disaster management. Quantitative, city-scale estimates of the expected economic and human losses are a prerequisite for that shift. They inform retrofit prioritisation, insurance and risk-transfer instruments, land-use planning and emergency preparedness.

Probabilistic seismic risk assessment (PSRA) combines a seismic hazard model, an exposure model and vulnerability or fragility functions to estimate loss metrics such as the average annual loss (AAL), probable maximum losses and annual fatalities (Silva et al. 2014; Silva et al. 2020). Open tools such as the OpenQuake engine (Pagani et al. 2014) and openly available global fragility and vulnerability models (Martins and Silva 2021) now allow such assessments to be carried out in regions without locally calibrated models, as illustrated by national-scale applications in the Himalaya (Chaulagain et al. 2015). However, every component of the chain carries epistemic uncertainty, and the literature has repeatedly shown that the choice between equally defensible models can change risk metrics by a factor of several (Crowley et al. 2005; Baker and Cornell 2008; Kalakonas et al. 2020). Analytical fragility and vulnerability models, in particular, remain an important source of this uncertainty (Silva et al. 2019). For human losses, the uncertainty is compounded by the step that converts structural damage into casualties. Empirical, semi-empirical and analytical casualty models differ in the damage state they condition on, in the assumed occupancy at the time of the event and in the lethality of collapse (ATC 1985; Coburn and Spence 2002; Jaiswal and Wald 2010; Spence et al. 2011; So and Spence 2013; FEMA 2024).

Peshawar, the provincial capital of Khyber Pakhtunkhwa (KP), illustrates the problem. The district hosts more than 4.3 million people, most of whom live in non-engineered unreinforced brick and adobe masonry. Experimental, analytical and field studies have repeatedly confirmed the high seismic vulnerability of the unreinforced brick, stone and adobe masonry that dominates housing in Pakistan (Korkmaz 2009; Mahmood and Ingham 2011; Ahmad et al. 2012; Ali et al. 2013). It lies about 30 km from the Main Boundary Thrust and about 200

km from the Hindu Kush intermediate-depth seismic zone. Previous loss estimates for Peshawar span more than three orders of magnitude, from 0.2 to 0.3 fatalities per year (Khan et al. 2018) to several hundred per year (Khan et al. 2025). They also rely on superseded hazard models or on 1998 census exposure data (Ahmad et al. 2014; Khan et al. 2018). Published 475-year peak ground acceleration (PGA) values for the city range from 0.06 g to 0.40 g (Rafi et al. 2012; Waseem et al. 2018; Mahmood et al. 2020; Waseem et al. 2020). Such scatter makes it difficult for decision makers to know which estimate to trust and which assumptions matter most.

In a preliminary conference contribution (Khan et al. 2025), the authors presented an event-based PSRA of Peshawar's residential buildings using the 2021 Building Code of Pakistan (BCP-2021) hazard model, a 2017-census based exposure model and GEM fragility functions. That study reported an AAL of USD 22.8 million and 412 to 881 fatalities per year. The present paper goes substantially beyond that preliminary analysis. It interrogates, decomposes and tests those estimates, and its specific contributions are:

(i) a hazard-consistent closed-form surrogate of the event-based model, obtained by inverting the aggregate loss-exceedance curve into an equivalent hazard curve and verified against the building-code hazard and 13 independent hazard studies;

(ii) the identification and correction of a systematic bias in the casualty step, namely treating the complete-damage state of analytical fragility functions as collapse, and a comparison of five casualty-model configurations;

(iii) a nine-factor tornado analysis and a 1,500-realisation Monte Carlo propagation of epistemic uncertainty in hazard, fragility, damage-to-loss, vulnerability-model version, replacement cost, occupancy, collapse fraction and lethality;

(iv) an independent back-analysis of the 26 October 2015 Mw 7.5 Hindu Kush earthquake and a benchmark against the GEM global risk model; and

(v) a typology-specific benefit-cost and cost-per-life-saved analysis of seismic retrofitting.

The remainder of the paper is organised as follows. Section 2 reviews previous risk studies for Peshawar. Section 3 describes the models and the uncertainty framework. Section 4 presents the results, Section 5 discusses their implications and limitations, and Section 6 concludes.

2 Study area and previous loss estimates

District Peshawar lies in the Peshawar basin, bounded by the Main Boundary Thrust to the south and by the Hindu Kush-Pamir deep seismic zone to the north-west. Recent damaging events include the 1992 Mw 6.3 Shakkar Khel (Kohat) earthquake and the 26 October 2015 Mw 7.5 Hindu Kush earthquake, which occurred at a depth of about 210 km and produced a PGA of 0.053 g in Peshawar (Ahmad 2015). That event caused localised damage in the city, including roof collapses in the old city and the failure of a masonry retaining wall at the Bala Hisar fort (Ahmad et al. 2019). Province-wide, it caused 232 deaths and damaged 97,995 houses (IFRC 2016). Peshawar was not among the nine worst-affected districts.

The district Peshawar comprises an urban core surrounded by northern and southern rural zones (Fig. 1). The urban core contains 41% of the buildings and 46% of the population, at a density of about 13 people per building, compared with about 11 in the rural zones.

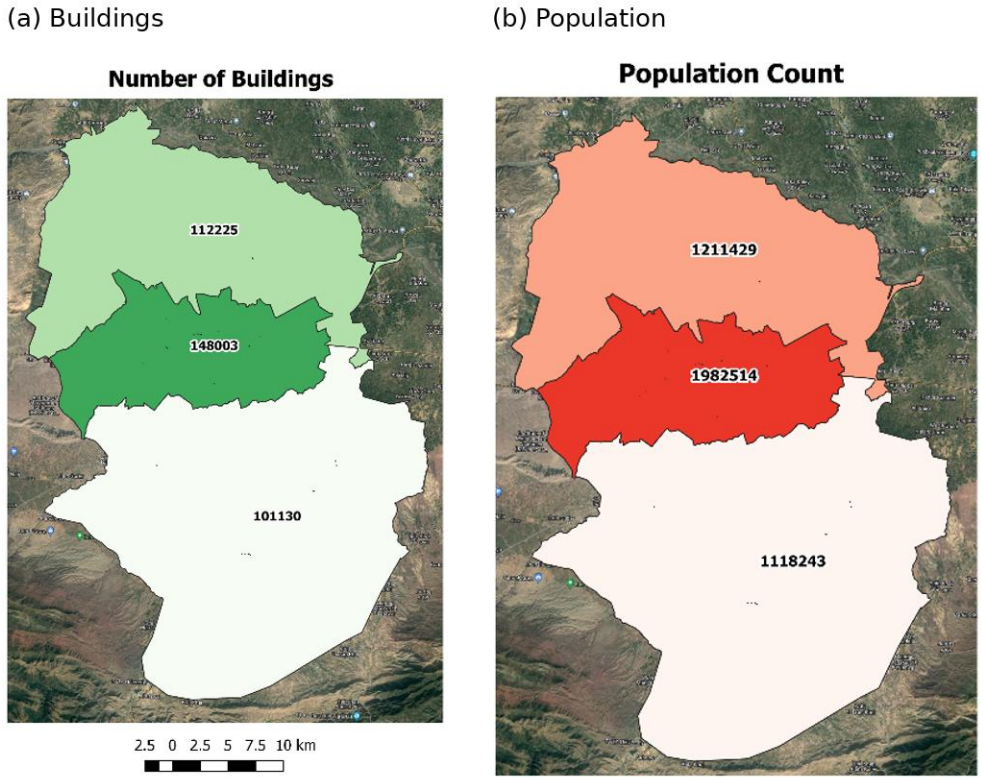


Fig. 1 District Peshawar and its exposure zones: (a) number of residential buildings and (b) population in the northern rural, urban and southern rural zones, based on the 2017 census (PBS 2017) as compiled by Hassan et al. (2022). Base imagery: Google Satellite

Table 1 summarises previous quantitative loss estimates that include Peshawar. They differ in hazard model, exposure data, typology resolution and loss metric, which precludes a direct comparison and motivates the uncertainty analysis in this paper.

Table 1 Previous seismic loss estimates covering Peshawar

Study	Hazard input	Exposure	Key result for Peshawar
Ahmad et al. (2014)	GSHAP global hazard model, classical PSHA	1998 census; 2 classes (kacha/pacca)	AAL USD 5 to 15 million
Khan et al. (2018)	Monte Carlo (EQRAM)	1998 census	USD 13 to 20 per building (475 yr); 0.2 to 0.3 deaths/yr
ADB (2021), GEM model	GEM global hazard model	GEM global exposure	KP province: AAL USD 145 million; 187 deaths/yr
Khan et al. (2025)	BCP-2021, event-based	2017 census; 7 GEM classes	AAL USD 22.8 million; 412 to 881 deaths/yr
This study	BCP-2021 + equivalent hazard; literature range	As above, plus GEM v2026 alternative	AAL USD 20.2 to 22.8 million; 51 to 77 deaths/yr (central)

3 Methodology

3.1 Framework

The analysis proceeds in two stages (Fig. 2). In Stage 1, an event-based probabilistic damage and loss calculation is performed with the OpenQuake engine (v3.19) using the hazard, exposure and fragility models described in Sections 3.2 to 3.4. In Stage 2, the event-based output is used to calibrate a transparent closed-form model (Section 3.5). That model then serves three purposes: re-deriving damage-state statistics with alternative consequence models (Section 3.6), propagating epistemic uncertainty (Section 3.7), and evaluating a historical scenario and retrofit options (Sections 3.8 to 3.9).

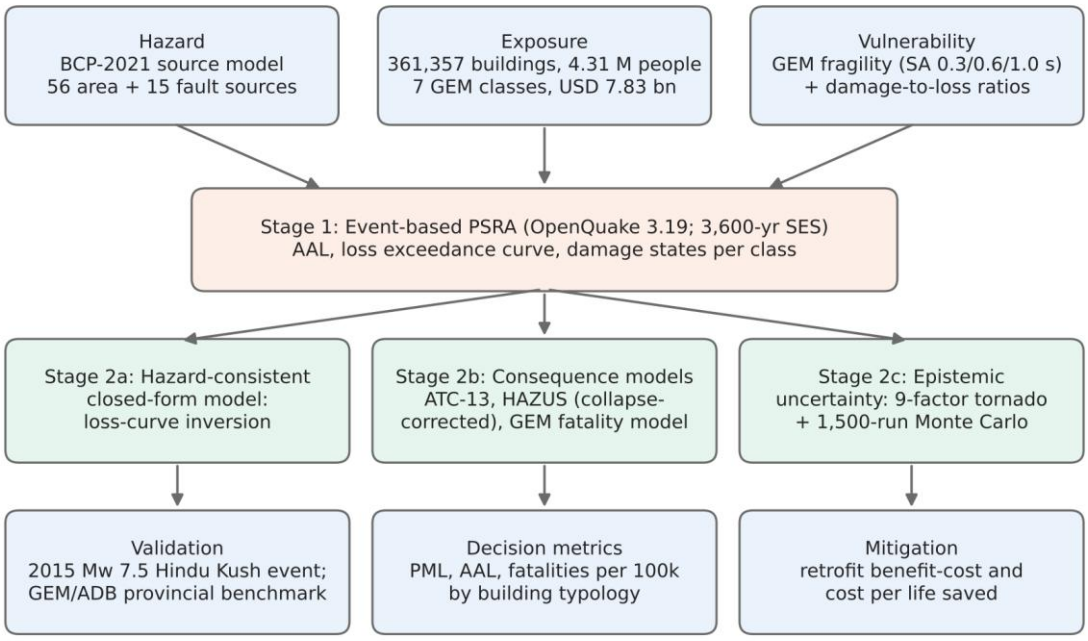


Fig. 2 Two-stage framework adopted in this study. Stage 1 is the event-based PSRA; Stage 2 derives a hazard-consistent closed-form model used for consequence-model comparison, uncertainty propagation, validation and mitigation analysis

3.2 Seismic hazard model

The hazard model is the source model developed for BCP-2021 (PEC 2021), comparable in scope to other national probabilistic hazard models for Pakistan (Rafi et al. 2012; Waseem et al. 2020). It contains 7,386 declustered events distributed over 56 area sources: 47 shallow crustal, four deep, one subduction intraslab and four subduction interface sources. It also includes 15 characteristic fault sources (Fig. 3). Seismicity in each area source follows a truncated Gutenberg-Richter recurrence, $\log_{10}N = a - bM$ (Gutenberg and Richter 1944), with minimum magnitude Mw 4.0 and source-specific maximum magnitudes between Mw 5.5 and 9.2. Fault sources are characteristic, with minimum magnitudes of Mw 6.5 to 6.9. Sources within 250 km of the district were retained. Site amplification was represented by Vs30 values derived from topographic slope (Wald and Allen 2007), a proxy whose accuracy depends on the resolution of the topographic data and on the geological setting (Allen and Wald 2009). A stochastic event set equivalent to 3,600 years of seismicity (111,062 events) was generated, and ground-motion fields were computed for SA(0.3 s), SA(0.6 s) and SA(1.0 s), the intensity measures of the fragility functions. BCP-2021 gives short-period and 1-s spectral accelerations for Peshawar of S_S = 0.83 g and S_1 = 0.29 g on reference rock (2% probability of exceedance in 50 years).

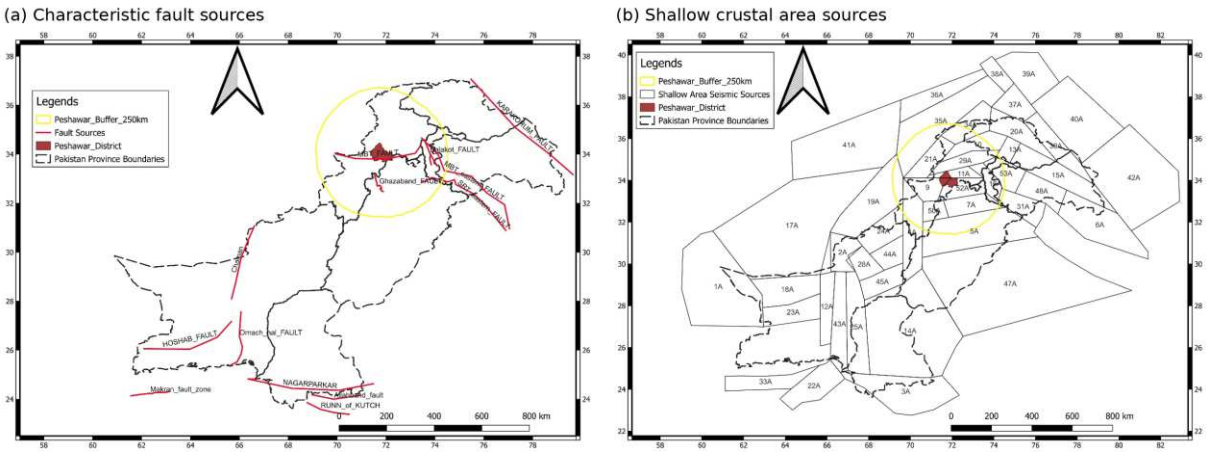


Fig. 3 BCP-2021 seismic source model: (a) characteristic fault sources and (b) shallow crustal area sources. The yellow circle marks the 250-km integration distance around District Peshawar (dark red). Source geometries from the BCP-2021 hazard model (PEC 2021); maps prepared by the authors

3.3 Exposure model

The exposure model follows Hassan et al. (2022), who mapped the dwelling attributes of the 2017 Population and Housing Census (PBS 2017) (wall material, roof material, construction period) to 25 residential typologies using the GEM building taxonomy, field observations and expert judgement. It separates an urban core (148,003 buildings; 1,982,514 people) from northern and southern rural zones (213,355 buildings; 2,329,672 people). Because analytical fragility functions are not available for every one of the 25 typologies, these were consolidated into the seven GEM classes listed in Table 2. Replacement costs were derived from average built-up areas (100 to 250 m^2 per building) and unit costs of PKR 24,000 to 32,000 per m^2, based on the KP Market Rate System 2021, adjusted by 5 to 10% downward for rural areas and inflated by 30% to 2022 prices. The resulting total replacement value is PKR 2,106 billion (USD 7.83 billion at 269 PKR/USD). Unreinforced brick masonry (56.0% one-storey; 8.9% two-storey) and adobe (21.2%) dominate the inventory (Fig. 4).

Table 2 Building classes, counts, replacement values and fragility intensity measures (IM)

Class (GEM taxonomy)	Buildings	Share (%)	Value (USD M)	Fragility IM
URM-B 1st (MUR+CLBRS/LWAL+DNO/H1)	202,465	56.0	4,794.4	SA(0.3 s)
URM-B 2st (MUR+CLBRS/LWAL+DNO/H2)	32,058	8.9	835.1	SA(0.3 s)
CM 2st (MCF/LWAL+DUM/H2)	9,695	2.7	287.0	SA(0.3 s)
Adobe 1st (MUR+ADO/LWAL+DNO/H1)	76,534	21.2	1,146.6	SA(0.3 s)
RC-I 3st (CR/LFINF+CDL+DUM/H3)	157	0.0	3.7	SA(0.6 s)
RC-I 5st (CR/LFINF+CDL+DUM/H5)	15,045	4.2	356.3	SA(1.0 s)
Timber 1st (W+WBB/LFM+CDN/H1)	25,403	7.0	380.6	SA(0.3 s)
Total	361,357	100.0	7,803.6	

Note: class-level replacement values are reconstructed from the average built-up areas and unit costs above. Their sum differs by 0.4% from the total exposure value used in the event-based run.

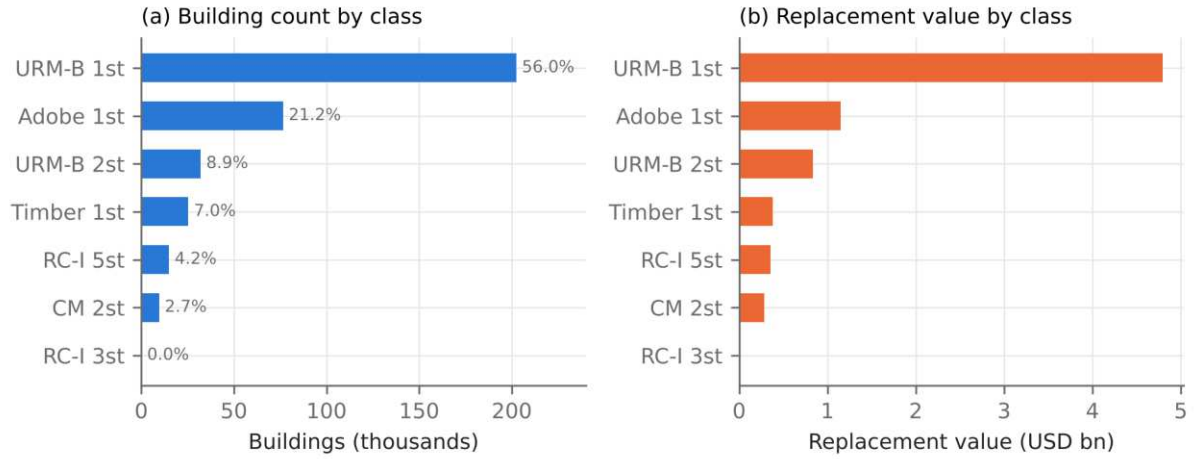


Fig. 4 Composition of the residential exposure model: (a) number of buildings and (b) replacement value per building class. Building counts derived from the exposure model of Hassan et al. (2022)

3.4 Fragility and damage-to-loss models

Fragility functions for the seven classes were taken from the GEM global fragility and vulnerability model (Martins and Silva 2021). It defines four damage states: slight (DS1), moderate (DS2), extensive (DS3) and complete (DS4). The functions are lognormal in a class-specific spectral acceleration. Damage was converted to structural loss with the GEM damage-to-loss ratios of 0.05, 0.20, 0.60 and 1.00 for DS1 to DS4 (Martins and Silva 2021). The probability of being in damage state k at intensity x is

$$p(DS_k \mid x) = P(DS \geq DS_k \mid x) - P(DS \geq DS_{k+1} \mid x), \quad P(DS \geq DS_k \mid x) = \Phi[\, \ln(x / \theta_k) / \beta_k \,] \tag{1}$$

where θ_k and β_k are the median and logarithmic standard deviation of damage state k, Φ is the standard normal CDF and $P(DS \geq DS_5) = 0$. The mean loss ratio of class j follows as

$$LR_j(x) = \Sigma_{k=1..4}\, DLR_k \cdot p(DS_k \mid x) \tag{2}$$

3.5 Hazard-consistent closed-form model

The event-based run yields an aggregate loss-exceedance curve, a portfolio AAL and class-level damage statistics, but not the underlying hazard curve. To make the model transparent and to enable rapid uncertainty propagation, an *equivalent* hazard curve $\lambda(s)$ is derived for s = SA(0.3 s). For each return period T of the event-based aggregate curve, the intensity s_T is found such that the value-weighted portfolio loss ratio equals the event-based loss ratio $LR_{agg}(T)$:

$$\Sigma_j\, V_j \cdot LR_j(r_j\, s_T) \,/\, \Sigma_j\, V_j = LR_{agg}(T) \tag{3}$$

Here V_j is the replacement value of class j and r_j converts SA(0.3 s) to the class intensity measure through the BCP-2021 design-spectrum shape (r = 1.0, 0.58 and 0.35 for SA(0.3 s), SA(0.6 s) and SA(1.0 s)). The pairs (s_T, 1/T) for T ≥ 5 years are fitted with a quadratic in log-log space, i.e. a second-order hazard approximation (Vamvatsikos 2013):

$$\ln \lambda(s) = c_0 + c_1 \ln s + c_2 (\ln s)^2 \tag{4}$$

This gives c_2 = -0.375, c_1 = -3.228 and c_0 = -7.568. Because the district is small relative to the source-to-site distances, a single equivalent curve represents the portfolio. Annual metrics then follow from the hazard integral

$$E[Y_j] = \int y_j(s)\, |d\lambda(s)| \tag{5}$$

where $y_j(s)$ is the class-level conditional metric: the loss $V_j \cdot LR_j(s)$, the expected number of buildings in damage state k, $N_j \cdot p(DS_k|s)$, or the expected number of fatalities (Section 3.6). The fragility functions were digitised for the dominant class (one-storey unreinforced brick, MUR+CLBRS/LWAL+DNO/H1). The fitted medians are 0.33, 0.68, 1.08 and 1.35 g for DS1 to DS4, with dispersions of 0.53 to 0.65. Combined with Eq. 2, they reproduce the published GEM vulnerability function of that class within 0.05 in loss ratio. For the other classes, the same fragility shape was scaled by a factor α_j fitted to the class GEM vulnerability function by least squares. The root-mean-square error was ≤0.021 for the six masonry and RC classes and 0.10 for the timber class, whose contribution to risk is negligible.

3.6 Consequence models for fatalities

Fatalities are estimated as the number of occupants multiplied by a damage-state-conditional lethality:

$$F_j = O_j \cdot f_{occ} \cdot \Sigma_k N_{j,k} \cdot L_k \quad (6)$$

Here O_j is the number of occupants per building (11.9 on average), f_{occ} is the fraction present at the time of the earthquake, $N_{j,k}$ is the annual expected number of buildings in damage state k and L_k is the lethality. Five configurations are compared:

ATC-13, complete = collapse: L = 0.0001, 0.001, 0.01 and 0.20 for DS1 to DS4 (ATC 1985). This is the configuration used by Khan et al. (2025);

HAZUS, complete = collapse: L = 0, 0.00001, 0.0001 and 0.10 for DS1 to DS4, also as in Khan et al. (2025);

HAZUS, collapse-corrected: in HAZUS the 10% lethality applies only to the collapsed fraction of completely damaged buildings. That fraction is 15% for unreinforced masonry and low-rise concrete, 13% for mid-rise concrete and reinforced or confined masonry, and 3% for light wood frames. The non-collapsed remainder has a lethality of 0.0001 to 0.0002 (FEMA 2024). The DS4 lethality therefore becomes $L_4 = f_{col} \cdot 0.10 + (1 - f_{col}) \cdot 0.0002$;

ATC-13, collapse-corrected: the same collapse fractions applied with the ATC-13 rates (0.20 for collapse, 0.01 otherwise);

GEM fatality vulnerability: the fatality vulnerability functions of the GEM global model for Pakistan (Martins and Silva 2021), integrated directly over the hazard curve.

The distinction matters because the complete-damage state of analytical fragility functions is defined by a displacement-capacity threshold. It is not equivalent to physical collapse, which in post-earthquake surveys affects only a fraction of completely damaged buildings (Jaiswal et al. 2011; So and Spence 2013; FEMA 2024).

Fig. 5 shows the two pathways from complete damage to fatalities. In the conventional pathway, every building in DS4 is treated as collapsed and the collapse lethality is applied to all its occupants. In the corrected pathway, only the collapsed fraction carries collapse lethality, and the remainder carries the much lower lethality of complete damage without collapse.

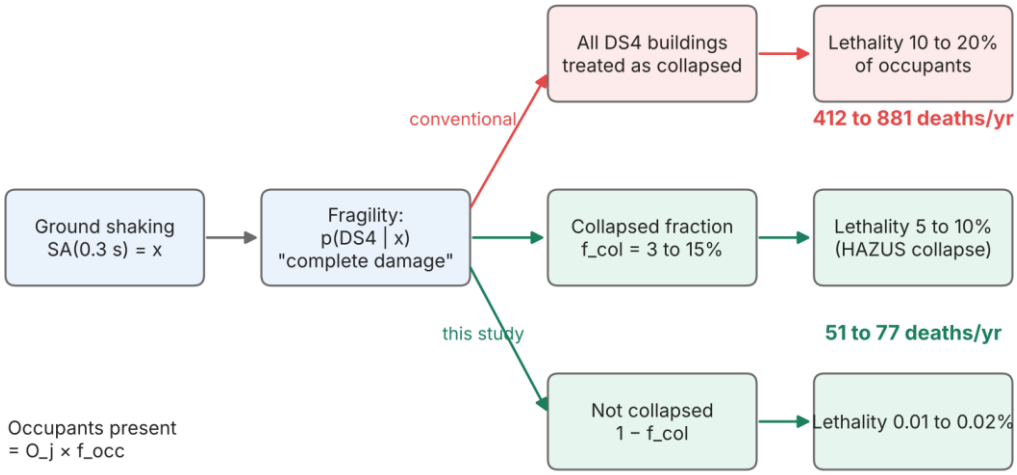


Fig. 5 Event tree of the casualty step from complete damage (DS4) to fatalities, contrasting the conventional assumption (complete damage = collapse) with the collapse-corrected formulation adopted in this study. Collapse fractions and lethality rates from FEMA (2024) and ATC (1985); annual fatality ranges are results of this study

3.7 Treatment of epistemic uncertainty

Nine sources of epistemic uncertainty were considered (Table 3). The hazard was varied by scaling the equivalent hazard curve so that the implied 475-year PGA spans 0.20 to 0.38 g, the central range of the 13 studies compiled by Mahmood et al. (2020). An SA(0.3 s)/PGA ratio of 2.25 was used. Fragility capacity was varied by ±20% in median. The damage-to-loss ratios were varied between the GEM values and HAZUS-type values (0.02, 0.10, 0.50, 1.00). The vulnerability model was switched between the GEM release used in Stage 1 (v2021) and the current Pakistan-specific GEM release (v2026.0.0; GEM 2026a), whose masonry functions are conditioned on PGA. Replacement cost was varied between the values of the GEM global

exposure model for KP (Yepes-Estrada et al. 2023; GEM 2026b), i.e. USD 183 per m^2 and 70 m^2 per building or 59% of the present value, and +20%. The fatality-related factors (occupancy, collapse fraction, lethality and casualty model) enter only the human-loss estimate. One-at-a-time variations produce tornado diagrams, a common screening tool for ranking the contributions of epistemic inputs to loss uncertainty (Baker and Cornell 2008; Kalakonas et al. 2020). A Monte Carlo simulation with 1,500 realisations samples all factors simultaneously (uniform distributions over the ranges in Table 3; equal weights for discrete alternatives) to obtain distributions of AAL and annual fatalities. The vulnerability-model version is kept out of the Monte Carlo and reported as a separate scenario because its effect is a structural model change rather than a parametric range.

Table 3 Epistemic factors, ranges and the metric they affect

Factor	Central value	Range / alternatives	Affects
Hazard level (475-yr PGA)	0.28 g (equivalent)	0.20 to 0.38 g	AAL, fatalities
Fragility capacity (median)	GEM v2021	×0.80, ×1.25	AAL, fatalities
Damage-to-loss ratios	GEM (0.05/0.2/0.6/1.0)	HAZUS-type (0.02/0.1/0.5/1.0)	AAL
Vulnerability model version	GEM v2021	GEM v2026.0.0 (SA/PGA 2.0 to 2.5)	AAL (scenario)
Replacement cost	USD 7.8 bn	×0.59 (GEM exposure), ×1.20	AAL
Occupancy at time of event	100%	55 to 100%	Fatalities
Collapse fraction of DS4 (masonry)	15%	10 to 20%	Fatalities
Lethality of collapse	10%	5 to 20%	Fatalities
Casualty model	HAZUS collapse-corrected	GEM fatality; ATC-13 collapse-corrected	Fatalities

3.8 Validation and benchmarking

Two independent checks were performed. First, the 2015 Mw 7.5 Hindu Kush earthquake was simulated as a scenario with the recorded PGA of 0.053 g in Peshawar (Ahmad 2015), converted to SA(0.3 s) with a ratio of 2.25. Within-district ground-motion variability was represented by a lognormal distribution with $\sigma = 0$ to 0.6. The predicted damage and deaths were compared with the observed provincial toll (232 deaths in all of KP; IFRC 2016) and with the absence of Peshawar from the list of severely affected districts. Second, annualised results were benchmarked against the GEM/ADB country risk profile, which reports an earthquake AAL of USD 145.3 million and 187 annual deaths for KP (ADB 2021).

3.9 Retrofit benefit-cost analysis

Retrofitting was modelled as an increase in fragility capacity by a factor $\gamma = 1.3$, 1.5 or 2.0 for one- and two-storey brick masonry and adobe, spanning an assumed range from light, low-cost strengthening to substantial upgrading of masonry houses. The benefit is the present

value of the AAL reduction over a 50-year life at a 10% discount rate (annuity factor 9.91). The benefit-cost ratio (BCR) is computed for retrofit costs of 10% and 20% of replacement value, following the approaches of Smyth et al. (2004) and Kappos and Dimitrakopoulos (2008). The net cost per statistical life saved is the retrofit cost minus the present value of avoided losses, divided by the discounted number of avoided deaths (collapse-corrected HAZUS model).

4 Results

4.1 Equivalent hazard and consistency with independent hazard studies

Fig. 6 shows the equivalent SA(0.3 s) hazard curve obtained by inverting the event-based loss curve. The fitted curve gives SA(0.3 s) = 0.63 g at 475 years and 1.08 g at 2,475 years. The 2,475-year value is within 12% of the BCP-2021 S_S (0.83 g on rock) amplified by a site factor of 1.17 (0.97 g). The implied 475-year PGA of about 0.28 g lies in the middle of the 0.20 to 0.38 g range of independent studies (Waseem et al. 2018; Mahmood et al. 2020). The hazard embedded in the event-based model is therefore neither anomalously high nor anomalously low, so any overestimation of losses must arise elsewhere in the chain. Integrating the GEM vulnerability functions over the equivalent hazard curve reproduces the event-based AAL (USD 22.7 vs. 22.8 million). The fragility-reconstructed closed-form model gives USD 20.2 million (−11%), which is adopted as the baseline for the uncertainty analysis.

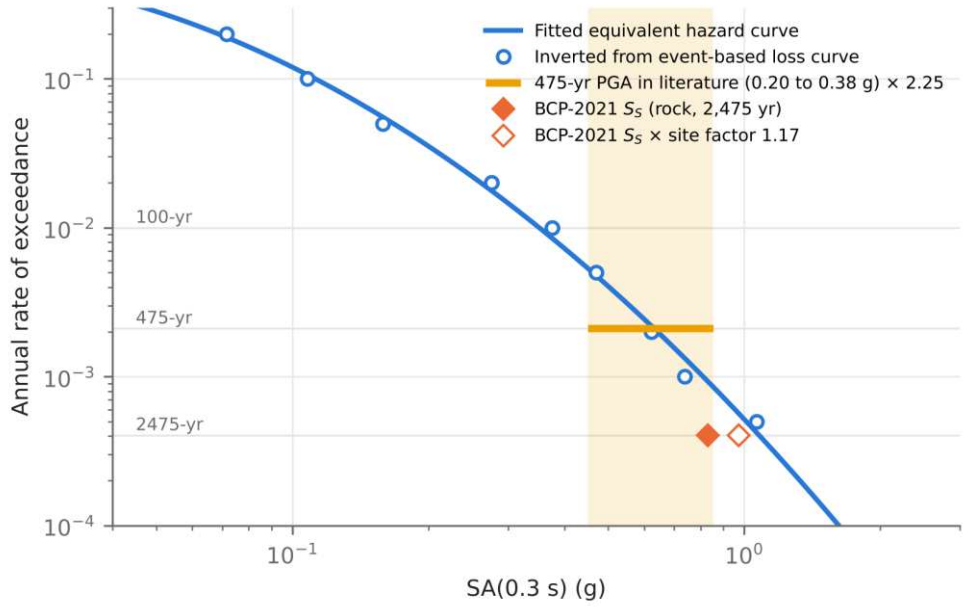


Fig. 6 Equivalent SA(0.3 s) hazard curve for District Peshawar inverted from the event-based aggregate loss curve (circles) and fitted with Eq. 4 (line). It is compared with the BCP-2021 2,475-year short-period

acceleration (PEC 2021) and with the range of 475-year PGA values published for Peshawar (Mahmood et al. 2020), converted with SA(0.3 s)/PGA = 2.25

4.2 Economic losses

The event-based aggregate loss-exceedance curve (Fig. 7) gives probable maximum losses of USD 0.48 billion (6.2% of replacement value) at 100 years, 1.38 billion (17.6%) at 475 years and 3.54 billion (45.2%) at 2,000 years. Class-level results from the closed-form model (Table 4; Fig. 8) show that one-storey brick masonry (55%) and adobe (31%) account for most of the AAL. Adobe has the highest loss ratio (5.5‰ per year), more than twice that of brick masonry (2.3 to 2.5‰). Unreinforced masonry as a whole accounts for 97% of the AAL. In the event-based run, two-storey urban brick masonry contributed a larger share than in the closed-form model (USD 6.6 vs. 2.1 million). This is consistent with higher per-building values of urban two-storey houses, which the district-average values in Table 2 do not capture.

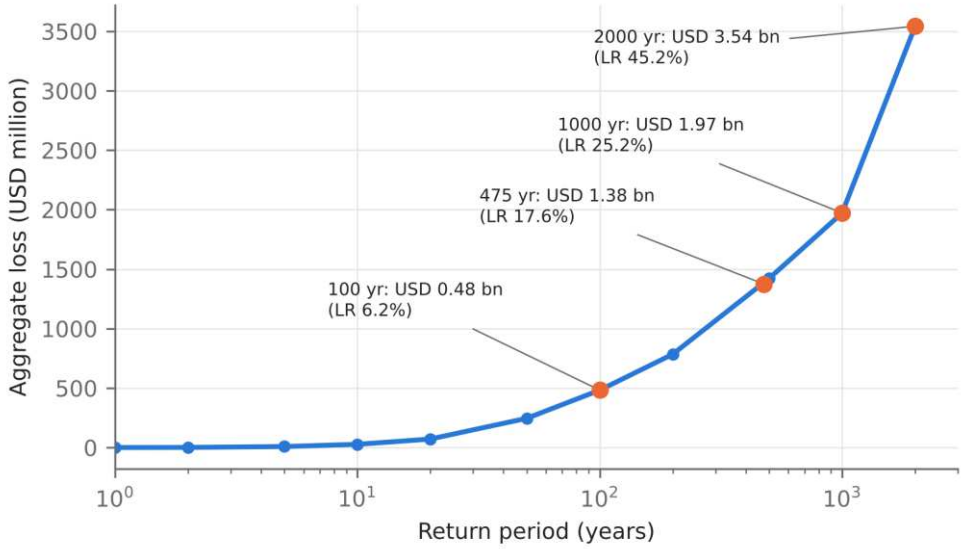


Fig. 7 Aggregate structural loss-exceedance curve for the residential building stock of District Peshawar from the event-based analysis, with probable maximum losses at selected return periods

Table 4 Annualised results of the closed-form model by building class (baseline). DS4 = complete damage; collapses use the HAZUS collapse fractions

Class	AAL (USD M)	AALR (‰)	DS4 (bldg/yr)	Collapse (bldg/yr)	Deaths HAZUS-corr.	Deaths GEM	Deaths ATC-13-corr.
URM-B 1st	11.22	2.34	120.2	18.0	21.9	6.0	77.5
URM-B 2st	2.10	2.52	20.9	3.1	3.8	1.6	13.4
CM 2st	0.12	0.43	0.6	0.1	0.1	0.1	0.4
Adobe 1st	6.28	5.48	133.1	20.0	24.3	68.7	81.3
RC-I 3st	0.00	1.24	0.0	0.0	0.0	0.0	0.0
RC-I 5st	0.50	1.40	4.6	0.6	0.7	0.6	2.9
Timber 1st	0.02	0.06	0.1	0.0	0.0	0.0	0.1
Total	20.25	2.59	279.7	41.8	50.9	77.0	175.6

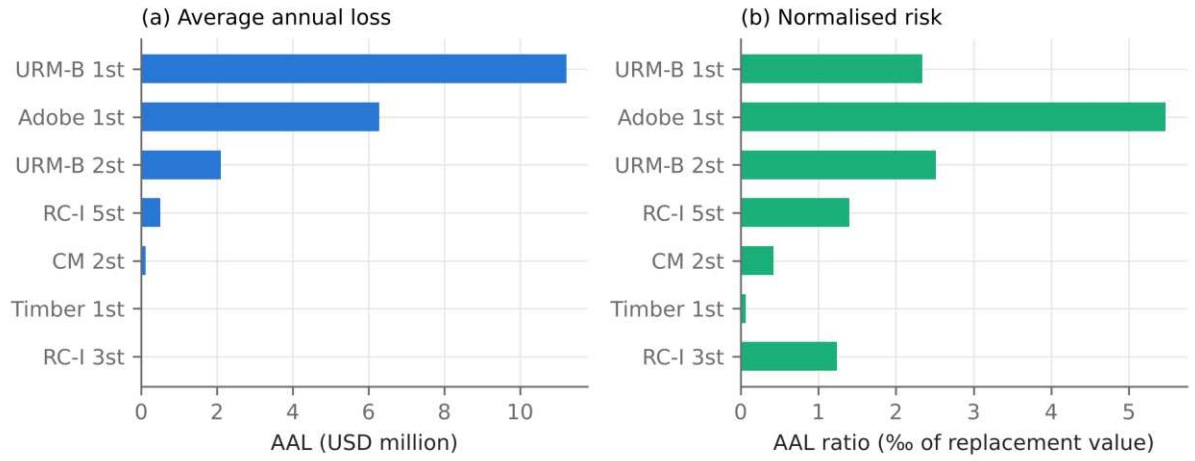


Fig. 8 Closed-form average annual loss (a) and average annual loss ratio (b) per building class

For the timber (W+WBB) and three-storey RC classes, which together account for 6.5% of the event-based AAL, the event-based run produced higher losses and complete-damage counts than the GEM functions of the same taxonomy imply. This indicates that the fragility functions mapped to these two classes in the event-based input should be re-examined. Because both classes are minor contributors, the portfolio conclusions are unaffected. The class-level results reported here use the GEM functions directly.

4.3 Damage and fatalities: the dominant role of the casualty step

The closed-form model predicts 280 buildings per year reaching complete damage, close to the 381 reported for the event-based run, of which about 42 are expected to physically collapse. Fig. 9 compares the annual fatalities obtained with the five consequence-model configurations. When complete damage is equated with collapse, the closed-form model yields 715 (ATC-13) and 334 (HAZUS) deaths per year. These values are consistent with the 881 and 412 obtained in the event-based run and confirm that the surrogate reproduces that run. Restricting collapse lethality to the collapsed fraction reduces the estimates to 176 (ATC-13) and 51 (HAZUS) deaths per year. The independent GEM fatality vulnerability functions give 77. The corrected estimates are thus five to eight times lower than those of the preliminary study.

Brick masonry and adobe account for 98% of the corrected HAZUS fatalities. The GEM fatality model attributes 89% of deaths to adobe, which is substantially more lethal than brick masonry in that model (up to 5% of occupants killed at high intensity, compared with 0.6 to 0.8% for brick masonry). Expressed per capita, the corrected estimates correspond to 1.2 to 1.8 deaths per 100,000 people per year. This is still 2.7 to 4 times the KP-wide average

implied by the GEM global model (0.44 per 100,000; ADB 2021), which is consistent with the higher replacement values and hazard near the Main Boundary Thrust. In contrast, the uncorrected estimates would imply that Peshawar alone experiences two to five times the annual fatalities of the entire province.

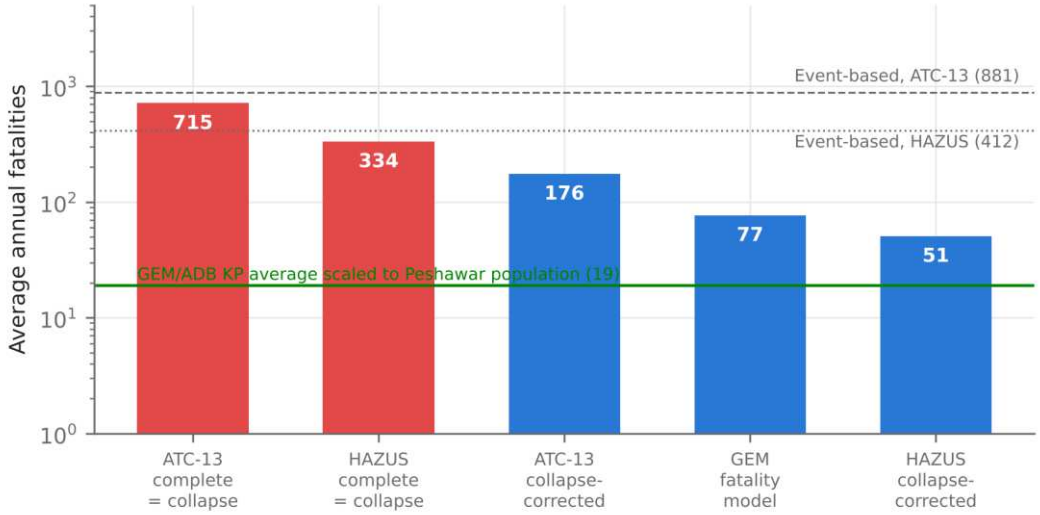


Fig. 9 Average annual fatalities for five consequence-model configurations (closed-form model). Red: complete damage treated as collapse, as in the preliminary study; blue: collapse-corrected or independent models. Dashed and dotted lines show the event-based values of the preliminary study (Khan et al. 2025), and the green line shows the KP average of the GEM model (ADB 2021) scaled to Peshawar's population

4.4 Epistemic uncertainty

The tornado diagrams (Fig. 10) rank the epistemic factors. For AAL, the hazard level is the most influential parametric factor (USD 9 to 39 million), followed by fragility capacity (USD 12 to 33 million). Replacement cost and damage-to-loss ratios each change AAL by up to 40%. The largest single change, however, comes from the version of the vulnerability model. The current Pakistan-specific GEM release lowers AAL to USD 3.0 to 6.0 million, a factor of four to seven, because its masonry functions are considerably less fragile at the intensities that dominate the hazard integral. For fatalities, the casualty model (51 to 176) and the hazard level (19 to 113) dominate, followed by collapse lethality, fragility capacity, collapse fraction and occupancy.

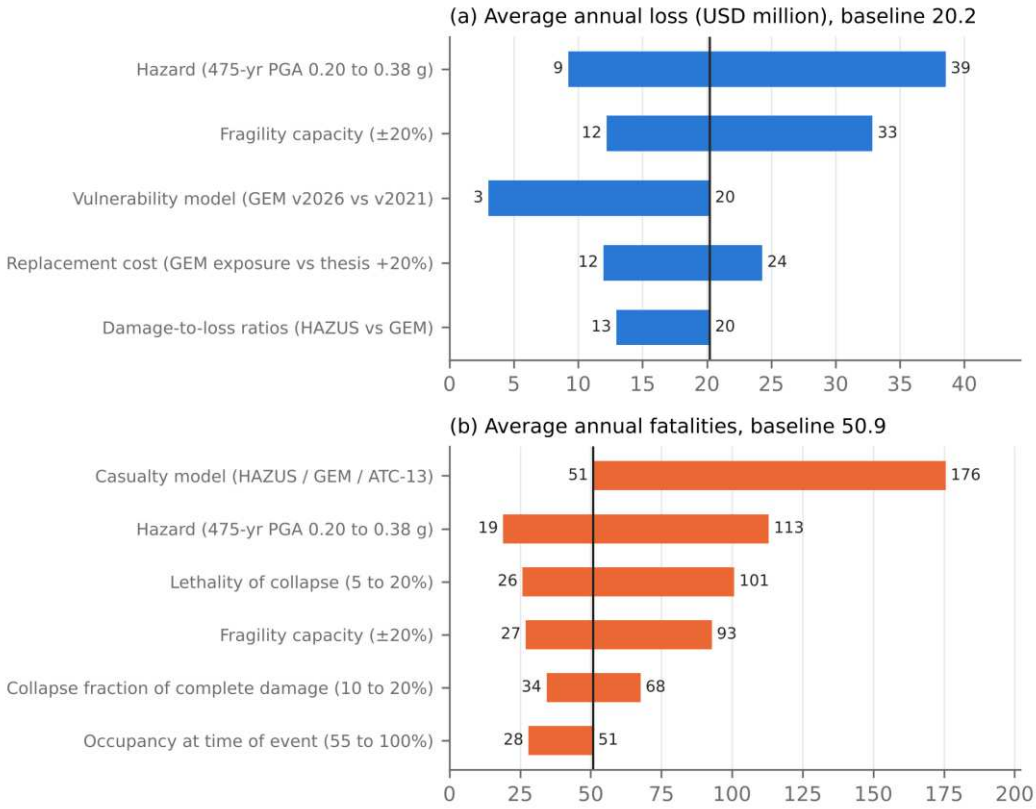


Fig. 10 Tornado diagrams of the one-at-a-time sensitivity of (a) average annual loss and (b) average annual fatalities (collapse-corrected HAZUS baseline). Bars span the results at the two ends of each range in Table 3

The Monte Carlo propagation (Fig. 11) gives a median AAL of USD 14.6 million with a 5 to 95% range of USD 5.1 to 35.9 million, and a median of 71 annual deaths with a 5 to 95% range of 18 to 259. The event-based AAL of the preliminary study (USD 22.8 million) lies near the 78th percentile and is therefore a plausible central-to-high estimate. Its fatality estimate of 412 per year, however, lies above the 95th percentile of the corrected distribution. The fatality distribution spans more than an order of magnitude between its 5th and 95th percentiles, so a single deterministic fatality figure for Peshawar should not be communicated without its uncertainty range.

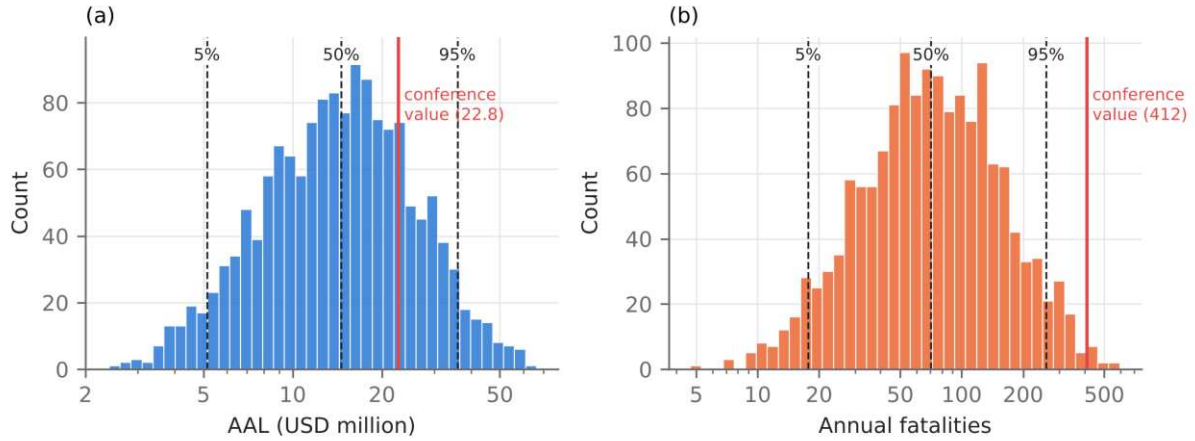


Fig. 11 Monte Carlo distributions (1,500 realisations) of (a) average annual loss and (b) average annual fatalities, with the 5th, 50th and 95th percentiles and the values of the preliminary event-based study

4.5 Validation against the 2015 Hindu Kush earthquake

Fig. 12 shows the deaths predicted in Peshawar for the 2015 Mw 7.5 Hindu Kush earthquake as a function of the assumed within-district variability of ground motion. With the recorded PGA of 0.053 g and moderate variability ($\sigma \leq 0.3$), the collapse-corrected model predicts 1 to 6 deaths, 22,000 to 27,000 slightly damaged buildings and at most a few collapses. This is consistent with the localised damage observed in the city and with Peshawar's absence from the list of severely affected districts. The complete-equals-collapse configuration predicts 5 to 37 deaths for the same range and exceeds the observed toll for the entire province (232) when σ approaches 0.5. Although the scenario check is limited by the single recorded PGA value, it independently supports the collapse correction.

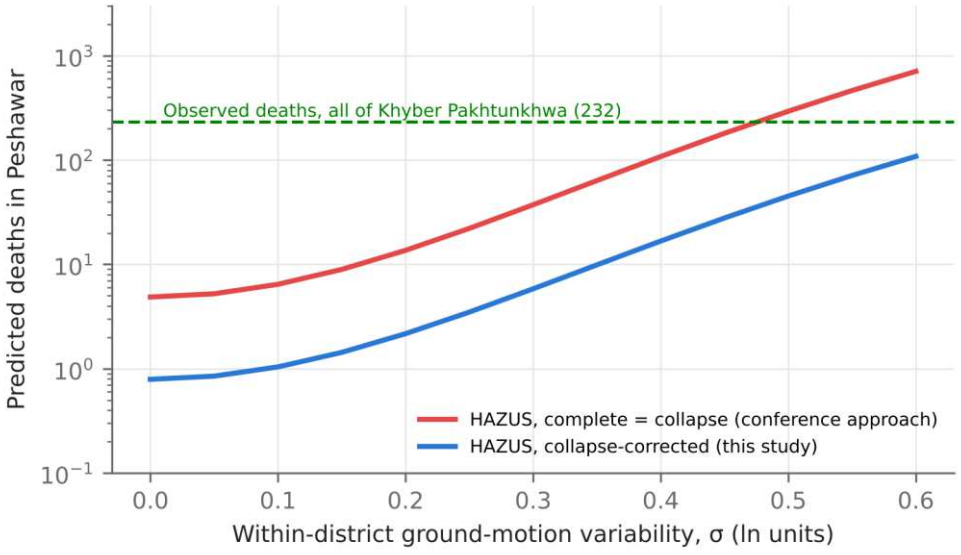


Fig. 12 Back-analysis of the 26 October 2015 Mw 7.5 Hindu Kush earthquake: deaths predicted in Peshawar as a function of within-district ground-motion variability, for the conference-paper approach and the collapse-corrected model, compared with the observed death toll in all of Khyber Pakhtunkhwa (IFRC 2016). The recorded PGA in Peshawar is from Ahmad (2015)

4.6 Retrofit benefit-cost and cost-effectiveness

Fig. 13 summarises the retrofit analysis. On direct economic losses alone, no retrofit option is justified. For a cost of 10% of replacement value, the BCR ranges from 0.11 to 0.19 for one-storey brick masonry and from 0.23 to 0.43 for adobe, depending on the capacity gain. This is typical of moderate-hazard settings in which the AAL ratio is a few per mille. When avoided deaths are considered, adobe retrofitting stands out. Its net cost per statistical life saved is USD 0.32 to 0.72 million, compared with USD 2.0 to 3.6 million for brick masonry, a five- to six-fold advantage. Under the GEM fatality model the advantage of adobe is even larger, because that model concentrates lethality in adobe. Retrofit programmes in Peshawar should therefore be justified mainly on life-safety grounds and should prioritise rural adobe housing.

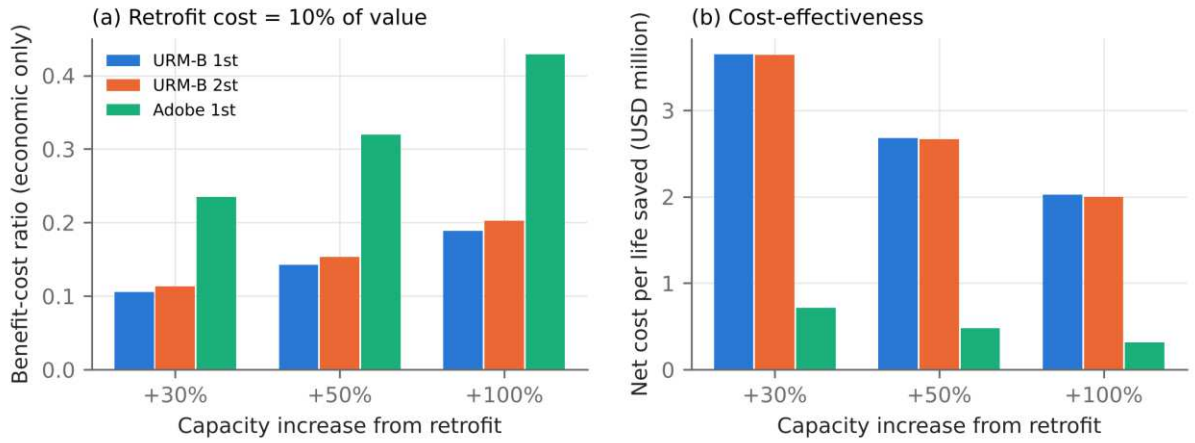


Fig. 13 Retrofit analysis for the three dominant classes: (a) economic benefit-cost ratio for a retrofit cost of 10% of replacement value and (b) net cost per statistical life saved (collapse-corrected HAZUS model, 50-year horizon, 10% discount rate)

5 Discussion

5.1 Why fatality estimates diverge

Previous estimates for Peshawar span 0.2 to 881 deaths per year (Table 1). This study shows that the spread is not random. The lower values of Khan et al. (2018) rely on 1998 exposure data and earlier hazard inputs, whereas the highest values arise from treating the complete-damage state of analytical fragility functions as collapse and applying collapse lethality to

every completely damaged building. Correcting that single step reduces the estimate five- to eightfold, more than any other factor considered. This pitfall is likely to be common, because OpenQuake consequence models and many regional studies define fatality ratios directly per damage state. A practical recommendation is therefore to state explicitly which physical outcome the highest damage state represents, and to apply collapse fractions (FEMA 2024) or empirically calibrated fatality vulnerability functions (Jaiswal and Wald 2010; Martins and Silva 2021) when the fragility functions are defined analytically.

5.2 Which uncertainties matter for decisions

For economic losses, the version of the vulnerability model produced a larger change than any parametric factor. This underlines that global models are periodically recalibrated and that results should state the model release. For fatalities, the casualty model, the hazard level and collapse lethality dominate, while occupancy and collapse fraction are second-order. Given limited resources, the most valuable investments in reducing uncertainty for Peshawar are therefore (i) post-earthquake collapse and casualty data for local masonry, to calibrate lethality, and (ii) a consensus hazard model at the city scale. Further refinement of the exposure model has less leverage for fatalities.

5.3 Limitations

The closed-form model uses a single equivalent hazard curve and neglects spatial variation of hazard and site conditions within the district. It also represents ground-motion variability only through the inversion. As a result, it reproduces portfolio averages well but is not intended for spatially resolved loss maps, and it does not capture the effect of spatial correlation of ground motion on the tail of the aggregate loss distribution (Weatherill et al. 2015). Fragility shapes for the non-dominant classes were inferred from published vulnerability functions rather than taken directly from the source fragility models. Class-level replacement values are district averages. Collapse fractions and lethality rates are taken from HAZUS and therefore reflect US construction, although their ranges were propagated as epistemic uncertainty. Finally, the 2015 back-analysis relies on a single recorded PGA value and on province-level casualty data, so it provides a consistency check rather than a formal calibration. A systematic comparison with historical earthquake loss databases (Daniell et al. 2011) is left for future work.

6 Conclusions

An updated probabilistic seismic risk model was developed for the residential buildings of District Peshawar, and its economic and human-loss estimates were decomposed and tested. The main conclusions are:

1. The hazard embedded in the BCP-2021 event-based model is consistent with the building code and with independent studies (equivalent 475-year PGA ≈ 0.28 g). The event-based AAL of USD 22.8 million (0.29% of replacement value) is a central-to-high estimate within a 5 to 95% epistemic range of USD 5 to 36 million.

2. Unreinforced brick masonry and adobe generate 97% of the AAL and 98% of the expected deaths. Adobe has the highest loss ratio (5.5‰ per year).

3. Treating complete damage as collapse inflates fatality estimates five- to eightfold. Collapse-corrected and independent models give 51 to 77 deaths per year (1.2 to 1.8 per 100,000), and the corrected model is consistent with the damage observed in Peshawar during the 2015 Hindu Kush earthquake.

4. The casualty model and the hazard level dominate the uncertainty in fatalities, while the vulnerability-model version dominates the uncertainty in AAL. Risk estimates for data-scarce cities should be reported with these sources of uncertainty made explicit.

5. Seismic retrofitting in Peshawar is not justified on direct economic losses alone. On life-safety grounds, adobe retrofitting is five to six times more cost-effective than retrofitting brick masonry and should be prioritised.

Declarations

Acknowledgements The authors thank the Earthquake Engineering Center, University of Engineering and Technology Peshawar, for computational resources, Waleed Hassan for the exposure model datasets, and the GEM Foundation for making the OpenQuake engine and the global fragility, vulnerability and exposure models openly available.

Funding The authors did not receive support from any organization for the submitted work.

Competing interests The authors have no relevant financial or non-financial interests to disclose.

Ethics approval Not applicable.

Declaration of generative AI and AI-assisted technologies Claude (Anthropic) was used for the compilation and arrangement of this manuscript. The authors reviewed and edited the content and take full responsibility for the content of the publication.

Author contributions Shahid Ullah: conceptualization, methodology, supervision, validation, writing, review and editing. Wasim Khan: conceptualization, methodology, software, formal analysis, investigation, data curation, visualization, writing, original draft. Both authors read and approved the final manuscript.

Data availability The GEM fragility, vulnerability and exposure models used in this study are openly available (Martins and Silva 2021; GEM 2026a; GEM 2026b). The OpenQuake input files, the event-based outputs and the scripts of the closed-form model, sensitivity analysis and Monte Carlo simulation are available from the corresponding author on reasonable request.

Prior presentation Preliminary Stage-1 results (event-based AAL and fatalities, without the analyses of Sections 3.5 to 3.9) were presented at the 3rd International Conference on Climate Resilient Infrastructure and Disaster Management (ICCRIDM-2025), UET Peshawar (Khan et al. 2025). The closed-form model, consequence-model comparison, uncertainty propagation, validation and retrofit analysis, and the corresponding text, figures and tables, are new.

References

ADB (2021) Country risk profile: Pakistan. Developing a disaster risk transfer facility in the Central Asia Regional Economic Cooperation region (TA-9878 REG). Asian Development Bank, Manila. https://carecprogram.org/uploads/CAREC-Risk-Profiles_Pakistan.pdf. Accessed 17 Oct 2026

Ahmad N (2015) A note on the strong ground motions and behavior of buildings during 26th Oct. 2015 Afghanistan–Pakistan earthquake. Earthquake Engineering Center, University of Engineering and Technology Peshawar, Peshawar. https://doi.org/10.13140/RG.2.1.3491.0802

Ahmad N, Ali Q, Ashraf M, Alam B, Naeem A (2012) Seismic vulnerability of the Himalayan half-dressed rubble stone masonry structures, experimental and analytical studies. Nat Hazards Earth Syst Sci 12(11):3441–3454. https://doi.org/10.5194/nhess-12-3441-2012

Ahmad N, Ali Q, Crowley H, Pinho R (2014) Earthquake loss estimation of residential buildings in Pakistan. Nat Hazards 73(3):1889–1955. https://doi.org/10.1007/s11069-014-1174-8

Ahmad N, Ullah S, Waseem M (2019) Discussion of "Assessment of the seismicity of Peshawar region in line with the historical data and modern building codes (ASCE-07 & IBC-2006)" by Shah et al. J Earthq Eng. https://doi.org/10.1080/13632469.2019.1692743

Ali Q, Khan AN, Ashraf M, Ahmed A, Alam B, Ahmad N, Javed M, Rahman S, Fahim M, Umar M (2013) Seismic performance of stone masonry buildings used in the Himalayan Belt. Earthq Spectra 29(4):1159–1181. https://doi.org/10.1193/091711EQS228M

Allen TI, Wald DJ (2009) On the use of high-resolution topographic data as a proxy for seismic site conditions (VS30). Bull Seismol Soc Am 99(2A):935–943. https://doi.org/10.1785/0120080255

ATC (1985) Earthquake damage evaluation data for California. Report ATC-13. Applied Technology Council, Redwood City, CA

Baker JW, Cornell CA (2008) Uncertainty propagation in probabilistic seismic loss estimation. Struct Saf 30:236–252. https://doi.org/10.1016/j.strusafe.2006.11.003

Bilham R (2009) The seismic future of cities. Bull Earthq Eng 7(4):839–887. https://doi.org/10.1007/s10518-009-9147-0

Chaulagain H, Rodrigues H, Silva V, Spacone E, Varum H (2015) Seismic risk assessment and hazard mapping in Nepal. Nat Hazards 78(1):583–602. https://doi.org/10.1007/s11069-015-1734-6

Coburn A, Spence R (2002) Earthquake protection, 2nd edn. John Wiley & Sons, Chichester

Crowley H, Bommer JJ, Pinho R, Bird J (2005) The impact of epistemic uncertainty on an earthquake loss model. Earthq Eng Struct Dyn 34(14):1653–1685. https://doi.org/10.1002/eqe.498

Daniell JE, Khazai B, Wenzel F, Vervaeck A (2011) The CATDAT damaging earthquakes database. Nat Hazards Earth Syst Sci 11(8):2235–2251. https://doi.org/10.5194/nhess-11-2235-2011

FEMA (2024) Hazus earthquake model technical manual, Hazus 6.1. Federal Emergency Management Agency, Washington, DC. https://www.fema.gov/sites/default/files/documents/fema_hazus-earthquake-model-technical-manual-6-1.pdf. Accessed 17 Oct 2026

GEM (2026a) Global Vulnerability Model, release v2026.0.0. GitHub. https://github.com/gem/global_vulnerability_model. Accessed 17 Oct 2026

GEM (2026b) Global Exposure Model, release v2026.0.0. GitHub. https://github.com/gem/global_exposure_model. Accessed 17 Oct 2026

Gutenberg B, Richter CF (1944) Frequency of earthquakes in California. Bull Seismol Soc Am 34(4):185–188. https://doi.org/10.1785/BSSA0340040185

Hassan W, Ullah S, Fahad M (2022) Exposure model development for Peshawar seismic risk assessment. In: Proceedings of the 2nd International Conference on Recent Advances in Civil Engineering and Disaster Management (ICCEDM-2022). Department of Civil Engineering, University of Engineering and Technology Peshawar, Peshawar, pp 161–165

IFRC (2016) Emergency plan of action final report. Pakistan: Earthquake 2015 (DREF operation MDRPK012). International Federation of Red Cross and Red Crescent Societies, Geneva. https://adore.ifrc.org/Download.aspx?FileId=141310. Accessed 17 Oct 2026

Jaiswal K, Wald DJ (2010) An empirical model for global earthquake fatality estimation. Earthq Spectra 26(4):1017–1037. https://doi.org/10.1193/1.3480331

Jaiswal K, Wald DJ, D'Ayala D (2011) Developing empirical collapse fragility functions for global building types. Earthq Spectra 27(3):775–795. https://doi.org/10.1193/1.3606398

Kalakonas P, Silva V, Mouyiannou A, Rao A (2020) Exploring the impact of epistemic uncertainty on a regional probabilistic seismic risk assessment model. Nat Hazards 104(1):997–1020. https://doi.org/10.1007/s11069-020-04201-7

Kappos AJ, Dimitrakopoulos EG (2008) Feasibility of pre-earthquake strengthening of buildings based on cost-benefit and life-cycle cost analysis, with the aid of fragility curves. Nat Hazards 45(1):33–54. https://doi.org/10.1007/s11069-007-9155-9

Khan SA, Pilakoutas K, Hajirasouliha I, Garcia R, Guadagnini M (2018) Seismic risk assessment for developing countries: Pakistan as a case study. Earthq Eng Eng Vib 17(4):787–804. https://doi.org/10.1007/s11803-018-0476-3

Khan W, Ullah S, Aman H (2025) Seismic risk estimation of residential buildings in district Peshawar. In: Proceedings of the 3rd International Conference on Climate Resilient Infrastructure and Disaster

Management (ICCRIDM-2025). Department of Civil Engineering, University of Engineering and Technology Peshawar, Peshawar, pp 404–412

Korkmaz KA (2009) Seismic safety assessment of unreinforced masonry low-rise buildings in Pakistan and its neighbourhood. Nat Hazards Earth Syst Sci 9(3):1021–1031. https://doi.org/10.5194/nhess-9-1021-2009

Mahmood H, Ingham JM (2011) Seismic vulnerability assessment of Pakistan unreinforced masonry buildings at a national scale. Seismol Res Lett 82(5):676–685. https://doi.org/10.1785/gssrl.82.5.676

Mahmood K, Ahmad N, Khan U, Iqbal Q (2020) Seismic hazard maps of Peshawar District for various return periods. Nat Hazards Earth Syst Sci 20(6):1639–1661. https://doi.org/10.5194/nhess-20-1639-2020

Martins L, Silva V (2021) Development of a fragility and vulnerability model for global seismic risk analyses. Bull Earthq Eng 19(15):6719–6745. https://doi.org/10.1007/s10518-020-00885-1

Pagani M, Monelli D, Weatherill G, Danciu L, Crowley H, Silva V, Henshaw P, Butler L, Nastasi M, Panzeri L, Simionato M, Vigano D (2014) OpenQuake engine: an open hazard (and risk) software for the Global Earthquake Model. Seismol Res Lett 85(3):692–702. https://doi.org/10.1785/0220130087

PBS (2017) Population and housing census 2017: district-wise results, Peshawar. Pakistan Bureau of Statistics. https://www.pbs.gov.pk/census-2017-district-wise/results/025. Accessed 17 Oct 2026

PEC (2021) Building Code of Pakistan (seismic provisions), 2021 edition. Pakistan Engineering Council, Islamabad. https://www.pec.org.pk/downloads-documents/building-code-of-pakistan/. Accessed 17 Oct 2026

Rafi Z, Lindholm C, Bungum H, Laghari A, Ahmed N (2012) Probabilistic seismic hazard of Pakistan, Azad-Jammu and Kashmir. Nat Hazards 61(3):1317–1354. https://doi.org/10.1007/s11069-011-9984-4

Silva V, Crowley H, Pagani M, Monelli D, Pinho R (2014) Development of the OpenQuake engine, the Global Earthquake Model's open-source software for seismic risk assessment. Nat Hazards 72(3):1409–1427. https://doi.org/10.1007/s11069-013-0618-x

Silva V, Akkar S, Baker J, Bazzurro P, Castro JM, Crowley H, Dolsek M, Galasso C, Lagomarsino S, Monteiro R, Perrone D, Pitilakis K, Vamvatsikos D (2019) Current challenges and future trends in analytical fragility and vulnerability modeling. Earthq Spectra 35(4):1927–1952. https://doi.org/10.1193/042418EQS101O

Silva V, Amo-Oduro D, Calderon A, Costa C, Dabbeek J, Despotaki V, Martins L, Pagani M, Rao A, Simionato M, Viganò D, Yepes-Estrada C, Acevedo A, Crowley H, Horspool N, Jaiswal K, Journeay M, Pittore M (2020) Development of a global seismic risk model. Earthq Spectra 36(1_suppl):372–394. https://doi.org/10.1177/8755293019899953

Smyth AW, Altay G, Deodatis G, Erdik M, Franco G, Gülkan P, Kunreuther H, Luş H, Mete E, Seeber N, Yüzügüllü Ö (2004) Probabilistic benefit–cost analysis for earthquake damage mitigation: evaluating measures for apartment houses in Turkey. Earthq Spectra 20(1):171–203. https://doi.org/10.1193/1.1649937

So E, Spence R (2013) Estimating shaking-induced casualties and building damage for global earthquake events: a proposed modelling approach. Bull Earthq Eng 11(1):347–363. https://doi.org/10.1007/s10518-012-9373-8

Spence R, So E, Scawthorn C (eds) (2011) Human casualties in earthquakes: progress in modelling and mitigation. Advances in Natural and Technological Hazards Research, vol 29. Springer, Dordrecht. https://doi.org/10.1007/978-90-481-9455-1

Vamvatsikos D (2013) Derivation of new SAC/FEMA performance evaluation solutions with second-order hazard approximation. Earthq Eng Struct Dyn 42(8):1171–1188

Wald DJ, Allen TI (2007) Topographic slope as a proxy for seismic site conditions and amplification. Bull Seismol Soc Am 97(5):1379–1395. https://doi.org/10.1785/0120060267

Waseem M, Lai CG, Spacone E (2018) Seismic hazard assessment of northern Pakistan. Nat Hazards 90(2):563–600. https://doi.org/10.1007/s11069-017-3058-1

582 Waseem M, Khan S, Khan MA (2020) Probabilistic seismic hazard assessment of Pakistan territory using an
583 areal source model. Pure Appl Geophys 177:3577–3597. https://doi.org/10.1007/s00024-020-02455-7

584 Weatherill G, Silva V, Crowley H, Bazzurro P (2015) Exploring the impact of spatial correlations and
585 uncertainties for portfolio analysis in probabilistic seismic loss estimation. Bull Earthq Eng 13:957–981.
586 https://doi.org/10.1007/s10518-015-9730-5

587 Yepes-Estrada C, Calderon A, Costa C, Crowley H, Dabbeek J, Hoyos MC, Martins L, Paul N, Rao A, Silva V
588 (2023) Global building exposure model for earthquake risk assessment. Earthq Spectra 39(4):2212–2235.
589 https://doi.org/10.1177/87552930231194048